ARTICLES

180° electron scattering from ^{14}C

M. A. Plum,* R. A. Lindgren,† J. Dubach, R. S. Hicks, R. L. Huffman,‡
B. Parker,§ and G. A. Peterson
University of Massachusetts at Amherst, Amherst, Massachusetts 01003

J. Alster, J. Lichtenstadt, and M. A. Moinester
School of Physics and Astronomy, Raymond and Beverly Sackler Faculty of Exact Science, Tel Aviv University, Tel Aviv, Israel 69778

H. Baer
Los Alamos National Laboratory, Los Alamos, New Mexico 87545
(Received 13 April 1989)

Inelastic electron scattering cross sections for ^{14}C have been measured at a scattering angle of 180°, with incident beam energies ranging from 81.9 to 268.9 MeV. Transverse form factors were measured for transitions to low-lying natural-parity states, to unnatural-parity "stretched" $J^\pi=4^-$ states, and to the $J^\pi=2^-$ analog to the ^{14}B ground state. Cross sections for 4^- states at 11.7 and 17.3 MeV are combined with pion scattering data to determine the isoscalar and isovector transition amplitudes. Form factors for other states are compared to shell-model calculations. From the excitation energy of the newly discovered $J^\pi T=2^-2$ state at 22.1 MeV, the ^{14}C-^{14}B Coulomb energy difference is determined to be 2.25 ± 0.10 MeV.

I. INTRODUCTION

Measurements of the transverse form factors for elastic and inelastic electron scattering from light nuclei ($4\leq A\leq 40$) have provided valuable information about the electromagnetic structure of nuclei but they have also left several intriguing puzzles. For example, the measured form factors for low-multipolarity transverse isovector excitations are generally much larger than the theoretical predictions at large momentum transfers. Also, studies of "stretched" parity-changing transitions (excitations of the highest multipolarity expected in the shell model) show that shell models systematically overestimate the observed cross sections. Whether the solutions to these puzzles are to be found in improved structure models or whether they involve as yet unknown excitation mechanisms remains an important open question.

Electron scattering measurements from ^{14}C may be of particular value in addressing this question. ^{14}C is the only even-even spin-0 neutron-excess ($T_0=1$) nucleus in the $1p$ shell whch can readily be used as a target. Thus the transverse excitations involve only one multipole but each may proceed through the strong isovector magnetization (spin) operator. In addition, in the extreme shell model, ^{14}C has a closed neutron shell, and the excitation of the low-lying positive-parity states may be expected to be simply interpreted as rearrangements of the protons within the p shell.

In this paper, therefore, we report measurements of 180° electron scattering cross sections for excitation of a number of states in ^{14}C (see Fig. 1). Transverse form factors have been extracted from these measurements over the momentum-transfer range $0.8\leq q\leq 2.8$ fm^{-1}. These data comprise the first measurement of the transverse form factors for excitation of some of these states and complement previous[4] measurements at lower q for the states at 6.091, 6.728, 7.012, and 8.318 MeV.

One main focus of this work is the determination of the "stretched" isoscalar and isovector $M4$ transition amplitudes for the excitation of the 11.7-, 17.3-, and 22.4-MeV 4^- levels. The interpretation of previous measurements[5] of $M4$ transitions in other p-shell nuclei such as ^{12}C is complicated because of substantial $T=0/1$ isospin mixing of the strong but broad and overlapping 4^- levels at 19.25 and 19.55 MeV. A similar isospin-mixing situation exists in ^{16}O among the weaker 4^- levels. This analysis is further complicated by large admixtures of $3p3h$ configurations which will make it difficult to interpret in terms of shell-model calculations. For ^{14}C the isospin mixing is expected to be weaker because the asymmetry energy provided by the spectator $p_{1/2}$ neutrons gives rise to a repulsive interaction which keeps the $T=1$ and $T=2$ levels from overlapping.

Electron scattering alone is insufficient to separate the isoscalar and isovector amplitudes contributing to the $M4$ excitations, so we turn to complementary information which can be obtained from previous measurements of inelastic pion scattering from ^{14}C to complete this separation. These results are then compared with shell-model calculations and provide an unusually detailed test of the ability of the model to calculate both the isoscalar and isovector amplitudes. In addition, we can then use these extracted amplitudes to predict (p,p') and (p,n) cross sections which, when measured, will provide a valu-

 ©1989 The American Physical Society

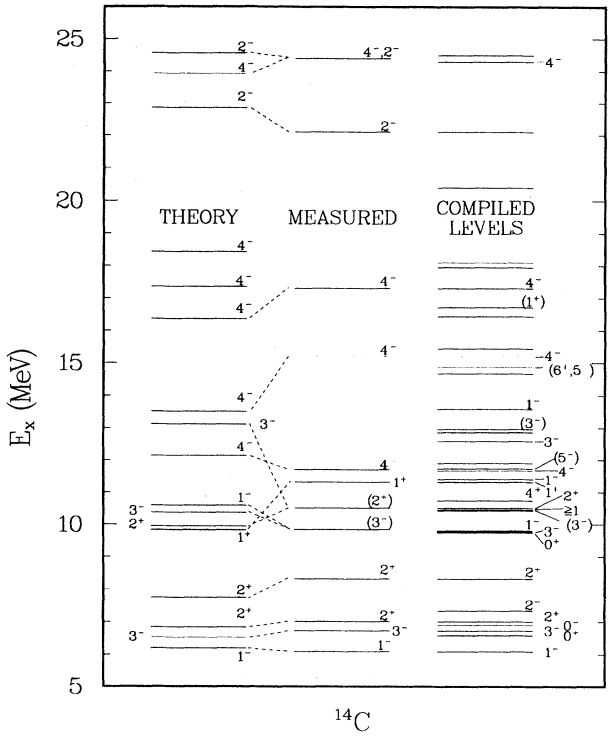

FIG. 1. Energy-level diagram for ^{14}C. The levels labeled "theory" are some of the levels predicted in the shell-model calculations of Ref. 1 and the $2\hbar\omega$ calculations reported here. The levels labeled "measured" are those for which form-factor data are presented. The compiled levels are taken from Refs. 2 and 3. ^{14}C has no known excited states below 6.091 MeV.

able test of the use of complementary probes to study the same transitions. A preliminary analysis of the 180° (e,e') measurements for the 4^- states has already been reported elsewhere;[4] in this paper new data and a more detailed analysis are presented.

A second objective of the present work is to obtain the form factors for the strong transverse electric transitions to natural-parity states in ^{14}C. In general such studies provide basic information on the magnetization and convection current densities where very little information is available. As discussed above, the low-lying excited states of ^{14}C can be accessed through the strong isovector operator and consequently are sensitive to the magnetization or spin density. This contrasts with weakly observed isoscalar transverse electric transitions to low-lying $T=0$ states in self-conjugate nuclei where the convection and magnetization currents make comparable contributions.

We compare the experimental form factors for the excitation of the negative-parity states with the same shell-model calculations[1] we used to describe the $M4$ transitions. To interpret the form factors for excitation of the positive-parity levels we have performed calculations in a full $2\hbar\omega$ shell-model space. Such calculations not only allow for rearrangements of the protons within the p shell, but also allow for excitation of both protons and neutrons out of the p shell. As we shall see, the shell-model calculations for both the positive- and negative-parity states have only mixed success in describing our data.

In Sec. II we discuss details of how the data were acquired. In Sec. III the plane-wave Born approximation is reviewed, and this is applied to the case of stretched transitions in Sec. IV. The other states are discussed in Sec. V, and finally, our conclusions are given in Sec. VI. The data set and the complete shell-model transition amplitudes have been submitted to the PAPS depository.[6]

II. EXPERIMENTAL DETAILS

The measurements were conducted at the Bates Linear Accelerator Center in Middleton, Massachusetts. Nine incident energies from 81.9 to 269.9 MeV were chosen to span the momentum-transfer range of 0.70 to 2.64 fm^{-1}. To maximize the sensitivity to transverse excitations, all measurements were taken at a scattering angle of 180° by using a system of four dipole magnets[7] and a 900-MeV/c split-dipole magnetic spectrometer.[8] The focal-plane instrumentation[9] for this spectrometer consisted of a drift chamber to measure the momentum of the scattered electrons, a pair of wire proportional counter arrays to limit the angular range transverse to the momentum dispersion plane, and two Cherenkov detectors to reduce background. Since the instrumented portion of the focal plane spanned a momentum bite of only 5%, several spectrometer field settings were necessary to acquire data over the 30-MeV range of excitation energies studied in this experiment.

The target consisted of a powder[4,10] with a ^{14}C/^{12}C atom ratio of 4.60±0.37. Since ^{14}C is radioactive, special precautions were taken to contain the powder. A target cell was constructed of 0.0025-cm stainless-steel foil windows brazed onto a 5 cm×9 cm U-shaped frame of 0.2-cm thick stainless steel. The space between the foils was packed with powder to a thickness of about 80 mg/cm^2. This cell was placed within another cell having 0.000 64-cm thick Havar[11] windows bolted in place. The upper portion of the target was closed by a porous sintered stainless-steel plug which allowed gases to escape during the evacuation of the scattering chamber without the loss of the radioactive powder. Because of the deleterious effects on glue of the intense radiation and heating due to beam currents as high as 30 μA, the only glue used in the target was on the plug.

Because of nonuniformities in the thickness of the powder and variations in the beam-spot position on the target, it was necessary to normalize the ^{14}C peaks to the peaks resulting from the ^{12}C contained in the target. The latter were in turn normalized to ^{12}C data obtained from a natural graphite target of known thickness. A dummy target consisting only of stainless steel and Havar foils was used to determine the background from the foil windows. Spectra for the ^{14}C target cell, the graphite target, and the dummy target for $E_0=166.7$ MeV are shown in Fig. 2. Also shown is the resultant ^{14}C spectrum after the ^{12}C and foil contributions were subtracted. Figure 3 shows the other ^{14}C spectra obtained after similar subtractions. A small unexpected hydrogen peak, perhaps due to a residue from the brazing of the target in a hydrogen furnace, is also seen in the spectra taken at lower energies.

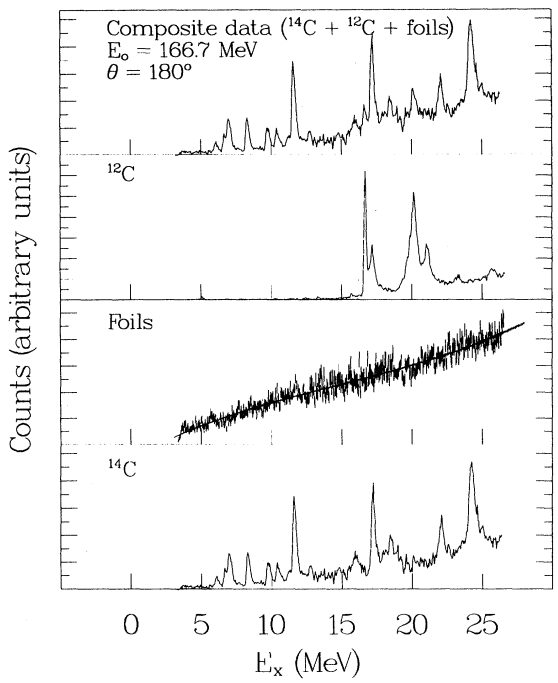

FIG. 2. The 166.7-MeV spectrum before and after subtracting the contributions of the foils and the admixtures of ^{12}C in the carbon powder. The foil spectrum shows a fit of a third-degree polynomial, with $1/\sigma^2$ weighting, used to subtract the foil background from the ^{14}C data.

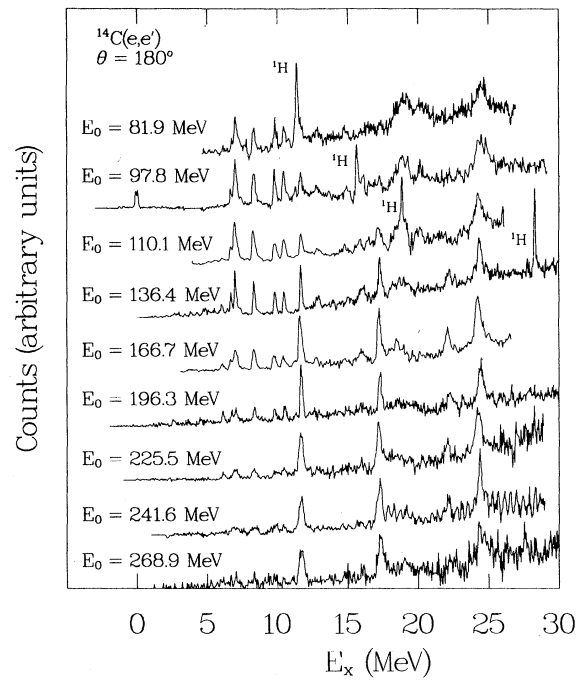

FIG. 3. The nine ^{14}C spectra obtained from this (e,e') experiment after subtraction of the foil and ^{12}C contributions. The vertical scale is different for each spectrum.

As a further normalization procedure, data were acquired with 20% momentum bite overlaps so as to determine relative bite-normalization factors, either from the ratio of areas under overlapping peaks, or from the ratio of sums of counts corrected for contributions from the foil windows. Errors in the bite normalization from the peak area method depend on the peak statistics and the number of peaks in the overlap region. Errors from the sums of counts method depend on the background statistics and the number of regions summed. Both techniques can be applied when peaks are present in the overlap region, thus reducing the relative bite-normalization error. On the average, the final error in the bite-normalization factors was estimated to be about 5%.

Cross sections were extracted from the bin-sorted data by least-squares fitting empirical line-shape functions that include radiation corrections[12] to the peaks. Because such a procedure will consistently underestimate the area under a peak when the data points are distributed according to a Poisson distribution,[13] the weights in the least-squares-fit procedure have been smoothed.[14] A portion of a fitted electron spectrum is shown in Fig. 4. The error bars shown in the following figures of form factors include uncertainties due to statistics from the line-shape fits, from relative bit normalizations, and from the normalization to known ^{12}C cross sections.

In principle, form factors deduced from cross sections measured at 180° are purely transverse. However, multiple-scattering effects and the finite solid angle subtended by the spectrometer aperture allow small contributions from longitudinal components. At an effective scattering angle of 177°, the shell-model calculations show that longitudinal components make up less than 5% of the measured cross section for the 6.091-, 6.728-, 7.012-, and 8.318-MeV states. Since the errors in the form factors typically range from 15 to 25 %, we make no attempt to subtract these minor longitudinal contributions to the data. States above 8.318 MeV that may be

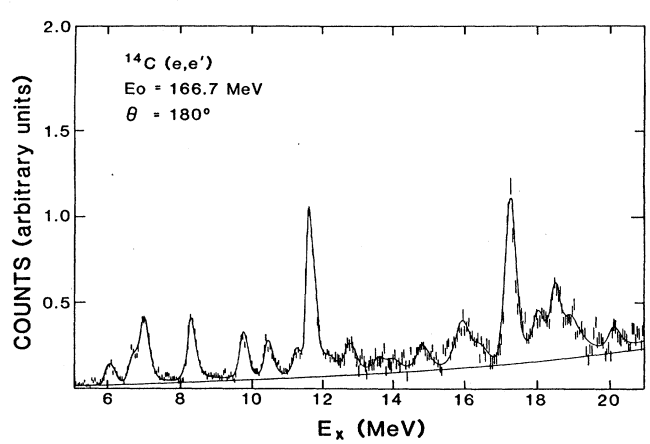

FIG. 4. An example of a fitted spectrum showing the fit to the (5–21)-MeV region of the spectrum obtained for an incident electron energy of 166.7 MeV. The underlying smooth line is a second-degree polynomial estimate of the background and radiation tails.

excited by electric transitions are not clearly resolved, and no estimates for the longitudinal contributions to these states have been made.

III. ELECTRON SCATTERING FORMALISM

In the plane-wave Born approximation (PWBA) the differential cross section for electrons scattered from a target nucleus is given by

$$\frac{d\sigma}{d\Omega}=\frac{Z^2\sigma_M}{\eta}\left[F_L^2(q)+\left[\frac{q_\mu^2}{2q^2}+\tan^2\frac{\theta}{2}\right]F_T^2(q)\right], \quad (1)$$

where the Mott-scattering cross section σ_M and the recoil factor η are given by

$$\sigma_M=\alpha^2\cos^2\frac{\theta}{2}\left[4E_0^2\sin^4\frac{\theta}{2}\right]^{-1}, \quad (2)$$

$$\eta=\left[1+\left[\frac{2E_0}{M}\right]\sin^2\frac{\theta}{2}\right]. \quad (3)$$

Z is the atomic number of the target nucleus, $\alpha=e^2/\hbar c=\frac{1}{137}$, θ is the laboratory scattering angle, E_0 is the incident electron energy, and M is the mass of the target nucleus. The four-momentum transfer q_μ is related to the three-momentum transfer q by $q_\mu^2=q^2-\omega^2$, where ω is the energy transferred to the nucleus. The nuclear structure information is then isolated in the longitudinal and transverse form factors $F_L^2(q)$ and $F_T^2(q)$.

Coulomb distortion corrections to the PWBA may be approximated by plotting the data as a function of effective momentum transfer,[15] given by

$$q_{\text{eff}}=q\left[1+\frac{3Ze^2}{2E_0R}\right], \quad (4)$$

where R is related to the mean-square radius $\langle r^2\rangle^{1/2}$ of the nucleus by $R=\frac{5}{3}\langle r^2\rangle^{1/2}$. For ^{14}C, $\langle r^2\rangle^{1/2}=(2.496\pm0.019)$ fm.[16]

For scattering from a spin-zero nucleus such as ^{14}C, only a single multipole, determined by the spin J of the excited state, will enter the cross section. In this case, the transverse form factor may be written[17,18]

$$F_T^2(q)=\frac{4\pi}{Z^2}(2J+1)\times\left|\frac{q\hbar}{2Mc}\sum_{\tau=0,1}\left[\tfrac{1}{2}g_\tau^s\rho_{J\tau}^{s\perp}(q)-2g_\tau^l\rho_{J\tau}^l(q)\right]^2\right|^2, \quad (5)$$

where τ is the rank of the isospin operator, g_τ^s and g_τ^l are the spin and orbital g factors, $\rho_{J\tau}^l$ is the diagonal-current transition density, and

$$\rho_{J\tau}^{s\perp}(q)=\left[\frac{J+1}{2J+1}\right]^{1/2}\rho_{JJ-1\tau}^s(q)-\left[\frac{J}{2J+1}\right]^{1/2}\rho_{JJ+1\tau}^s(q) \quad (6)$$

is the transverse-spin transition density decomposed in terms of its orbital projections $\rho_{JL\tau}^s$. Assuming one-body operators in a shell-model pictue, $\rho_{J\tau}^l$ and $\rho_{JL\tau}^s$ are then

$$\rho_{J\tau}^l=\sum_{j_aj_b}Z_{J\tau}(j_aj_b)\sqrt{2}\hat{j}_a\hat{J}^{-1}\times\langle j_a\|q^{-1}j_J(qr)[Y_J(\hat{r})\times\nabla]^J\|j_b\rangle \quad (7)$$

and

$$\rho_{JL\tau}^s=\sum_{j_aj_b}Z_{J\tau}(j_aj_b)\sqrt{2}\hat{j}_a\hat{J}^{-1}\times\langle j_a\|j_L(qr)[Y_L(\hat{r})\times\sigma]^J\|j_b\rangle, \quad (8)$$

where the sum runs over single-particle orbits of angular momentum j_a and j_b, $\hat{j}=\sqrt{2j+1}$, and $Z_{J\tau}(j_aj_b)$ is the spectroscopic amplitude[19]

$$Z_{J\tau}(j_aj_b)=\langle J_fT_f\|[a_{j_a}^\dagger\times\tilde{a}_{j_b}]^{J\tau}\|J_i=0,T_i\rangle, \quad (9)$$

where this matrix element is reduced with respect to total angular momentum. With this definition, $Z_{J\tau}$ takes the value of unity for a simple isoscalar or isovector particle-hole excitation from a closed shell.

Finally, if the transition densities are to be constructed from the shell model, one must take into account the finite size of the nucleon. This is easily done by multiplying the "point densities" of Eqs. (7) and (8) by the nucleon density[20]

$$\rho_{\text{FS}}(q)=\frac{0.312}{1+q^2/6.0}+\frac{1.312}{1+q^2/15.02}+\frac{-0.709}{1+q^2/44.08}+\frac{0.085}{1+q^2/154.2}, \quad (10)$$

with q in fm^{-1}, before using them in Eq. (5). In addition, the transition densities calculated in the shell model are inappropriate since the model allows independent excitations of single-particle orbits without demanding that the nuclear center of mass remain fixed. This is a much more difficult problem, but it can be treated in an approximate way by multiplying the densities in Eqs. (7) and (8) by[21]

$$\rho_{\text{c.m.}}(q)=\exp\left[\frac{1}{A}\left[\frac{qb}{2}\right]^2\right], \quad (11)$$

where b is the length parameter of a harmonic-oscillator approximation to the mean-field potential of the nucleus, and A is the number of nucleons in the nucleus. Such a treatment is not exact, but should be sufficient for our purposes.

IV. THE 4$^-$ STATES

As discussed in Sec. I, excitations of the 4$^-$ states in ^{14}C may be expected to have relatively simple interpreta-

tions. If the 0^+ ground state is described within a p-shell model, and the spectrum of negative-parity states arises from $1\hbar\omega$ excitations out of the p shell, only the single-particle matrix element $1p_{3/2} \rightarrow 1d_{5/2}$ will contribute. Since such a single-particle transition allows the transfer of at most 3 units of orbital angular momentum, a transition with $J=4$ must also involve the nucleon spin. Thus $\rho^l_{J\tau}$ vanishes. Similarly, only the $\rho^s_{JJ-1\tau}$ term contributes to $\rho^s_{J\tau}$. Thus, the transverse form factor for these transitions reduces to

$$F_T^2(q)=\frac{4\pi}{Z^2}(2J+1)\left|\frac{q\hbar}{2Mc}\sum_{\tau=0,1}\left[\tfrac{1}{2}g^s_\tau Z_{J\tau}\left[\frac{J+1}{2J+1}\right]^{1/2}\tilde{\rho}^s_{J,J-1}(a,b;q)\right]\right|^2 , \tag{12}$$

with

$$\tilde{\rho}^s_{J,J-1}(a,b;q)=(-1)^{l_b}(4\pi J)^{-1/2}\sqrt{2}\hat{j}_a\hat{j}_b\langle j_a j_b \tfrac{1}{2}(-\tfrac{1}{2})|J0\rangle\langle n_a l_a|j_{J-1}(qr)|n_b l_b\rangle , \tag{13}$$

and $(n_a,l_a,j_a)=(1,2,\frac{5}{2})$, $(n_b,l_b,j_b)=(1,1,\frac{3}{2})$, and $J=4$. Here we have assumed, as we shall throughout this discussion, that the neutron and proton single-particle wave functions are the same; any differences between them would be reflected in an isospin dependence in $\tilde{\rho}^s_{J,J-1}$, arising from different proton and neutron radial wave functions.

It should be emphasized that the structure of the 4^- states in ^{14}C need not be particularly simple. Indeed, configuration mixing within the 1p shell along with a number of possible $1\hbar\omega$ negative-parity excitations will give rise to 24 4^- $T=1$ and five 4^- $T=2$ states in ^{14}C. However, by the arguments given above, excitation of these states by reactions such as electron scattering, which dominantly proceed through a one-body operator, remains relatively simple. The amplitudes of the Z coefficients determined later in this paper will contain the fragmentation information.

A. The 11.7- and 17.3-MeV $T=1$ states

In Fig. 5, the experimental form factors for the excitation of the 11.7- and 17.3-MeV $J^\pi=4^-$, $T=1$ states are compared to transverse form factors calculated using harmonic-oscillator single-particle wave functions. The harmonic-oscillator size parameter and the magnitude of the calculated form factor were varied to give the best fit to the data. The average of the harmonic-oscillator parameters required to fit both the 11.7- and 17.3-MeV data is $b=1.52\pm0.04$ fm, a value in good agreement with the simple $A^{1/6}$ rule[21] that has been found to agree remarkably well with values deduced for other stretched transitions throughout the periodic table. The 11.7- and 17.3-MeV form factors also have the same q dependence and harmonic oscillator parameter as the 4^- states[5,22] in ^{12}C and ^{13}C.

Agreement between the (e,e') data and the calculated $M4$ form factor is not a definitive identification of the 11.7- and 17.3-MeV levels as 4^- states. However, such an identification is consistent with (π,π') angular distributions and excitation functions.[23,24] In addition, large-basis shell-model calculations[1] predict two strong 4^-, $T=1$ states at 12.13 and 16.35 MeV; no lower-spin negative-parity states predicted in this excitation region are consistent with either the (e,e') data or (π,π') data.

Combining Eqs. (1) and (12), and assuming the neutron and proton single-particle wave functions are given by the harmonic-oscillator well with $b=1.52$ fm, the 180° cross section at the observed peak of the experimental form factor is simply

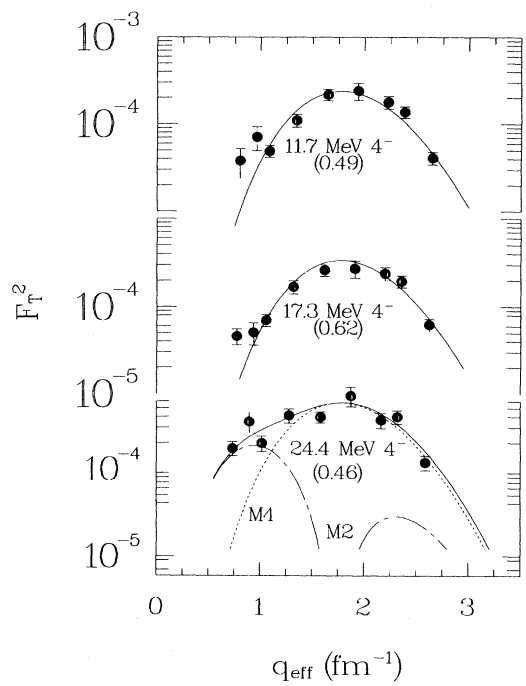

FIG. 5. Fit of the $(d_{5/2},p_{3/2})_{M4}$ form factor to data for the 11.7-MeV 4-state (top), 17.3-MeV 4^- state (middle), and 24.4-MeV complex (bottom). Numbers in parentheses are the normalization factors needed to fit the form factors predicted by the shell-model calculations of Ref. 1 to the data. For the 24.4-MeV complex, the dotted line shows the $(d_{5/2},p_{3/2})^{\Delta T=1}_{M4}$ form factor, the dot-dashed line shows the $M2$ form factor predicted by Millener and Kurath (Ref. 1), and the solid line gives the sum of these two contributions.

$$\left[\frac{d\sigma}{d\Omega}\right]_{\text{peak}}=(6.30\times10^{-34}\ \text{cm}^2)(g_0^sZ_0+g_1^sZ_1)^2\ , \qquad (14)$$

where we have suppressed all but the isospin labels on the Z's. The isoscalar and isovector magnetic moments are $g_0^s=0.88\ \mu_N$ and $g_1^s=-4.70\ \mu_N$, respectively. It is convenient to express this cross section in terms of the cross section for excitation of the 4^-, $T=1$ or $T=2$ states given by the extreme single-particle model (ESPM):

$$\left[\frac{d\sigma}{d\Omega}\right]_{\text{ESPM}}=(6.30\times10^{-34}\ \text{cm}^2)\times\{[1-(-1)^T][(g_0^s)^2/2]+(g_1^s)^2/2\}\ , \qquad (15)$$

where we have summed over the two degenerate 4^-, $T=1$ states. Thus the ratio of the experimental cross section to the ESPM cross section for excitation of the $T=1$ states is simply

$$\frac{d\sigma_{\text{peak}}/d\Omega}{d\sigma_{\text{ESPM}}/d\Omega}=\frac{\left[\sum_{\tau=0,1}g_\tau^sZ_\tau\right]^2}{[(g_0^s)^2+(g_1^s)^2/2]}\ . \qquad (16)$$

Table I shows the fraction of the ESPM cross section exhausted by the data shown in Fig. 5. Of course, the ESPM is naive and expected to overpredict the experimental strength. We therefore also show in Table I the ratio of the measured cross sections to those predicted in the more elaborate shell-model calculations of Ref. 1. As can be seen, these shell-model predictions are in better agreement with the data than the ESPM, but they still significantly overestimate the strength.

B. The 24.4-MeV $T=2$ state

The form factor for the peak at 24.4-MeV excitation is also shown in Fig. 5. This multipeak complex is comprised of a 4^- candidate and one or more unresolved states. A 4^- state at 24.4 MeV is consistent with the known[25] ^{14}B 4^-, $T=2$ state at 2.08±0.05 MeV, the ^{14}C analog of which is expected to lie at 24.2±0.1 MeV. This suggests a $T=2$ isospin assignment. Shell-model calculations[1] also predict a 4^-, $T=2$ state at 23.9 MeV. However, recent ^{14}C(π^-,γ) measurements[26] show a 2^-, $T=2$ state in ^{14}B at 2.15±0.17 MeV, the ^{14}C analog of which is expected to lie at 24.3±0.2 MeV. The shell-model $M2$ form factor for this level is peaked at low q, suggesting that the ^{14}C analog of the ^{14}B 2^- state is unresolved in our measurements and may be responsible for the rise in the (e,e') form factor below 1.3 fm^{-1}.

To account for a possible 2^- contaminant, we fit the data with the sum of the $(d_{5/2},p_{3/2}^{-1})_{M4}$ form factor and the predicted[1] $M2$ form factor. This fit required an $M4$ contribution that was (23±2)% of the ESPM, and an $M2$ normalization factor of 0.18. The error on the $M4$ contribution was obtained by least-squares fitting the $M4$ form factor to the six highest-q data points where the $M2$ contribution is expected to be weak, and fixing the harmonic-oscillator parameter to $b=1.52$ fm. Since only the isovector transition amplitude contributes to the excitation of the 4^-, $T=2$ state, this fit corresponds to [see Eqs. (14) and (15)]

$$Z_1=\sqrt{(0.40\pm0.03)/2}=0.45\pm0.02\ .$$

There are other cases of approximate degeneracy in the excitation energies of $T=T_0+1$, $J^\pi=4^-$ and 2^- levels involving the same particle-hole configurations. For example, in ^{12}C, the 4^- $T=1$ state at 19.6 MeV is unresolved from a 2^-, $T=1$ state with a dominantly $(d_{5/2},p_{3/2}^{-1})$ character.[22] Also in ^{16}O, there is a 4^-, $T=1$ state at 18.98 MeV and a 2^- candidate at 18.51 MeV with a form-factor shape consistent with a $(d_{5/2},p_{3/2}^{-1})$ configuration.[27] There is a similar situation in ^{24}Mg, where a 6^-, $T=1$ state at 15.13 MeV is nearby a 4^-, $T=1$ state at 15.54 MeV with a form-factor shape consistent with the $(f_{7/2},d_{5/2}^{-1})_{4^-}$ configuration.[28]

In addition to the experimental evidence for such a 4^-, 2^- degeneracy, the shell-model calculations of Ref. 1 also support this interpretation, predicting a 4^-, $T=2$ state at 23.92 MeV and a 2^-, $T=2$ state at 24.56 MeV with a predominatly $(d_{5/2},p_{3/2}^{-1})$ character. As in the case of the 4^-, $T=1$ states, however, the form factor predicted by the shell model is about a factor of 2 too large as shown in Table I.

TABLE I. Electron scattering cross sections at the peak of the form factor for the $J^\pi=4^-$ states in ^{14}C compared to extreme single-particle model (ESPM) and theoretical shell-model (theor) predictions[1] *without* and *with* meson exchange currents.

		$\frac{d\sigma_{\text{peak}}/d\Omega}{d\sigma_{\text{ESPM}}/d\Omega}\times100\%$		$\frac{d\sigma_{\text{peak}}/d\Omega}{d\sigma_{\text{theor}}/d\Omega}\times100\%$	
E_x (MeV)	T	Without	With	Without	With
11.7±0.1	1	18±1	15±1	56±3	49±3
15.2±0.1	1	<1.7	<1.5	<74	<64
17.3±0.1	1	25±1	22±1	72±4	62±4
24.4±0.1	2	46±4	40±3	53±4	46±4

C. Analysis of the 15.2-MeV state

A state at 15.2-MeV excitation was observed[23,24] with both $(\pi^+,\pi^{+\prime})$ and $(\pi^-,\pi^{-\prime})$ scattering, and was given a $J^\pi=4^-$ assignment. However, this state was not observed in our electron scattering experiment. The (e,e') cross section for this state can be estimated from the electorn scattering data to be at least 15 times smaller than the cross section for the 17.3 MeV 4^- state. Again, the shell-model calculations[1] are consistent with such an interpretation, predicting a weakly excited 4^- $T=1$ state at 13.50 MeV. As will be shown below, this is not inconsistent with the pion scattering results. For the ratio to the ESPM shown in Table I, however, the (e,e') data can only be used to set an upper limit.

D. Meson-exchange-current contributions

So far we have assumed that electron scattering proceeds solely as a one-body process. However, to accurately determine the one-body contributions, the small

but non-negligible effects of two-body meson-exchange currents (MEC) must be considered. Calculations[4] were performed for the stretched transitions in ^{14}C including pair, pionic, and nucleon-resonance-MEC terms. These were carried out using both simple particle-hole and configuration mixed shell-model wave functions, and in both cases inclusion of the MEC resulted in an increase in magnitude of about 15% at the maximum of the form factor. We have therefore assumed that the MEC contributions to strong stretched-states scale with the particle-hole amplitude. A PWBA harmonic-oscillator calculation with the various MEC contributions is shown in Fig. 6 for the first predicted[1] 4^-, $T=1$ state in ^{14}C. The pair, pionic, and N^* nucleon resonance MEC contributions are shown separately.

We have reanalyzed our data including an estimated 15% contribution from MEC. This tends to reduce the deduced one-body contribution which is to be compared to the ESPM and shell-model predictions. These new results are also shown in Table I.

We note that in previous work[5] it was shown that one-body strengths determined from calculations using Woods-Saxon radial wave functions (as opposed to harmonic-oscillator radial wave functions) are enhanced by about 20%, nearly canceling the 15% reduction caused by MEC. However, the calculations were done using bound wave functions, and more recent work[29] using unbound Woods-Saxon radial wave functions shows strong excitation-energy-dependent effects in the extracted one-body strengths. The best method of calculating one-body strengths is unclear at the moment, and we have therefore chosen to retain the harmonic-oscillator radial wave functions.

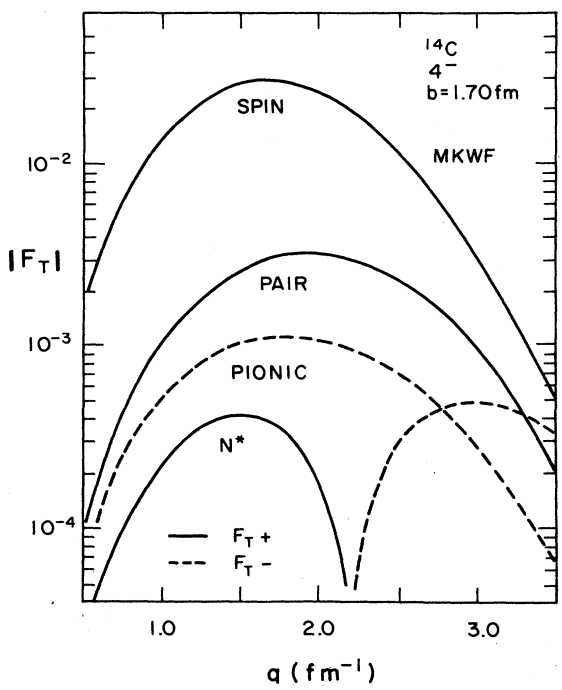

FIG. 6. The pair, pionic, and $N^*(3,3)$ MEC contributions to the $M4$ form factor obtained using the Millener-Kurath shell-model amplitudes (Ref. 1) (MKWF). A dashed line indicates destructive interference with the one-body ("spin") form factor, while a solid line indicates constructive interference.

E. Combined electron and pion analysis

1. *Analysis using (π,π') ratios*

For $T=1\rightarrow T=1$ transitions, electron scattering cross-section measurements alone are insufficient to separately determine the isoscalar and isovector one-body transition matrix elements. Since the isovector magnetic moment is over 5 times greater than the isoscalar magnetic moment, the (e,e') cross sections are usually dominated by the isovector spectroscopic amplitude Z_1. However, if Z_0 is comparable to or larger than Z_1, the contributions of the isoscalar amplitude cannot be neglected. In this section the ^{14}C(e,e') $M4$ cross sections will be taken together with the ratio of ^{14}C$(\pi^{\pm},\pi^{\pm'})$ cross sections for each state to give two independent equations which can be solved for the two unknowns Z_0 and Z_1. For the present case of ^{14}C, only the upper limits are known for the 11.7-MeV $(\pi^+,\pi^{+'})$ and 17.3-MeV $(\pi^-,\pi^{-'})$ cross sections. This leads to a range of values for the (π,π') ratios. Nevertheless, the pion-scattering data places strong limits on the values of the Z coefficients. This procedure is similar to that of Ref. 4, but in this case new data are included in the (e,e') form factors. While it is possible to determine the Z coefficients with greater precision by using pion-scattering cross-section calculations (see the following section) the results have larger unknown systematic errors due to the model dependence of the calculation.

The (π,π') cross section for excitation of the 4^- states in ^{14}C may be written[18] in a form analogous to Eq. (12):

$$\frac{d\sigma^{\pi}}{d\Omega} \propto \left[\sum_{\tau=0,1} t_{\tau}^{LS}(q) Z_{\tau} \rho^{s}_{J,J-1}(q) \right]^2 , \tag{17}$$

where t_0^{LS} (t_1^{LS}) is the isoscalar (isovector) pion-nucleus scattering amplitude. For π^+ (π^-) inelastic scattering at incident pion energies near the $N^*(3,3)$ resonance, $t_0^{LS}/t_1^{LS}=-2$ $(+2)$, and

$$R=\frac{d\sigma(\pi^+,\pi^{+'})}{d\sigma(\pi^-,\pi^{-'})}=\frac{[2(Z_0/Z_1)-1]^2}{[2(Z_0/Z_1)+1]^2} . \tag{18}$$

Note that in obtaining this ratio we have assumed that the q dependence of the isoscalar and isovector $\rho^{s}_{J,J-1,\tau}(q)$ is the same.

In the left half of Fig. 7, $1/R$ is shown as a function of Z_0/Z_1. For the 11.7-MeV state, the (π,π') data[24] require $1/R>17$, and Z_0/Z_1 is therefore confined to $0.31\le Z_0/Z_1\le 0.82$. From (e,e'),

$$(d\sigma_{\rm exp}/d\Omega)/(d\sigma_{\rm ESPM}/d\Omega)=0.15 ,$$

and Eq. (16) gives a second constraint on Z_0 and Z_1. This constraint may be recast to give Z_0 and Z_1 separately in terms of the ratio Z_0/Z_1, and these results are also

shown in Fig. 7 for the region consistent with the solution of Eq. (18). Combining the constraints from pion and electron scattering then requires $0.092 \le Z_0 \le 0.28$ and $0.30 \le Z_1 \le 0.34$, as may be seen in Fig. 7. Including the 6.1% error from the form-factor fit to the (e,e') data, $0.090 \le Z_0 \le 0.28$ and $0.29 \le Z_1 \le 0.35$. A similar analysis for the 17.3-MeV state is shown in the right half of Fig. 7, and the results for both states are summarized in Table II. The 11.7-MeV excitation is dominantly a neutron transition, and the 17.3-MeV excitation is dominantly a proton transition. Note that only the relative signs of Z_τ are determined here; the absolute signs are simply a matter of convention.

The uncertainties in the extracted Z coefficients are large because only upper limits have been measured for the 11.7-MeV $(\pi^+,\pi^{+\prime})$ and the 17.3-MeV $(\pi^-,\pi^{-\prime})$ cross sections, leading to large ranges in values for the pion cross-section ratios R. Because pion scattering is more sensitive to Z_0, it is this coefficient that has the largest error. In contrast, electron scattering is mainly sensitive to Z_1, leading to a smaller error for the Z_1 coefficient.

2. *Analysis using (π,π') cross sections*

A more model-dependent method of determining the nuclear-structure coefficients Z_0 and Z_1 relies on calculating pion-scattering cross sections. Such calculations are sensitive to both the form and details of the matter density. They also depend, to a lesser degree, on the type of transition (proton, neutron, isoscalar, or isovector), and the excitation energy. Unfortunately, as we will discuss, experience has shown that an empirical normalization factor is necessary to fit other pion-scattering data with such calculations. In what follows, the cross sections were calculated using the scattering potential code ALLWRLD (Ref. 30) and the distorted-wave (DW) code MSUDWPI.[31] A more complete description of these calculations may be found in Ref. 32.

The pion-scattering cross section at the peak of the angular distribution may be written

$$\frac{d\sigma_{\text{peak}}(\pi^+,\pi^{+\prime})}{d\Omega} = \frac{2(aZ_0 - Z_1)^2}{(a+1)^2} N^+ \sigma_{\text{DW}}^+ \tag{19}$$

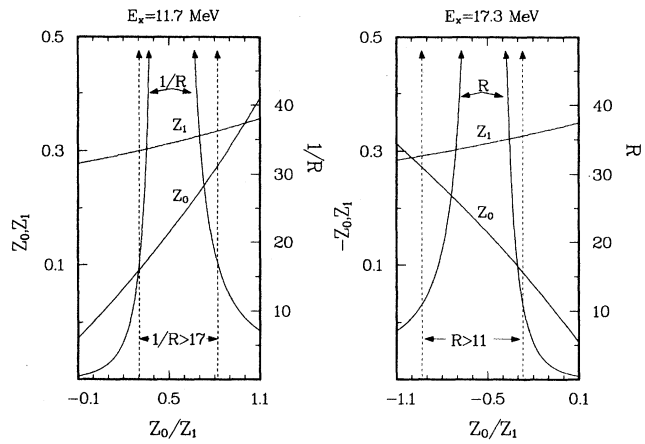

FIG. 7. Graphical solutions to Eqs. (14) and (18) for the 11.7- and 17.3-MeV states. R and $1/R$ curves are solutions to Eq. (18); Z_0 and Z_1 curves are solutions to Eq. (14).

and

$$\frac{d\sigma_{\text{peak}}(\pi^-,\pi^{-\prime})}{d\Omega} = \frac{2(aZ_0 + Z_1)^2}{(a+1)^2} N^- \sigma_{\text{DW}}^- \tag{20}$$

where a is the absolute value of the ratio of the isoscalar-to-isovector pion-nucleus scattering amplitude $|t_0^{LS}/t_1^{LS}|$, N^+ and N^- are empirical normalization factors, and $\sigma_{\text{DW}}^- = 414$ μb/sr is the differential cross section at the peak of the angular distribution calculated for a $(d_{5/2},p_{3/2}^{-1})$ $J^\pi = 4^-$ pure neutron transition ($Z_0 = Z_1 = 1/\sqrt{2}$) with $E_x = 11.7$ MeV. We choose to calculate σ_{DW}^- in this way because we know from the ratio analysis that the 11.7-MeV excitation is an almost pure neutron transition. Similarly, $\sigma_{\text{DW}}^+ = 435$ μb/sr is the differential cross section at the peak of the angular distribution calculated for a $(d_{5/2},p_{3/2}^{-1})$ $J^\pi = 4^-$ pure proton transition ($Z_0 = 1/\sqrt{2}$, $Z_1 = -1/\sqrt{2}$) with $E_x = 17.3$ MeV.

For a pion beam energy of 164 MeV, $a = 1.93$.[24,33] The factors N^+ and N^- were found[32] to be nearly equal for stretched transitions in ^{28}Si and ^{16}O, and are assumed to be equal here. Analysis of stretched 4^- transitions in

TABLE II. Results for the Z coefficients. Solutions from the method using pion cross sections give two solution sets. The disfavored sets are shown in parentheses.

E_x (MeV)	T	R[a]	Method using pion ratios Z_0	Method using pion ratios Z_1	Method using pion cross sections Z_0	Method using pion cross sections Z_1
11.7	1	$<1/17$	$0.09 \le Z_0 \le 0.28$	$0.29 \le Z_1 \le 0.35$	0.21 ± 0.01	0.32 ± 0.01
					(0.48 ± 0.01)	(-0.20 ± 0.01)
15.2	1	1.9 ± 0.6			0.22 ± 0.02	-0.07 ± 0.03
					(0.03 ± 0.02)	(-0.43 ± 0.03)
17.3	1	>11	$-0.28 \le Z_0 \le -0.08$	$0.28 \le Z_1 \le 0.34$	-0.32 ± 0.02	0.28 ± 0.01
					(0.72 ± 0.02)	(0.48 ± 0.01)
24.4	2			0.45 ± 0.02[b]		

[a]Values from Ref. 24.
[b]From electron scattering only. See the text.

^{16}O gave $N=N^{+}=N^{-}=1.30$,[32] and for the stretched 6^{-} transitions in ^{28}Si N was determined to be 1.15. For the $M4$ transitions in ^{13}C , value of $N\approx 1$ was used,[5] but in conjunction with Woods-Saxon radial wave functions. It is not clear to what degree the value of N depends on the type of radial wave functions used and the nucleus in question. In any case, both ^{16}O and ^{14}C involve the $1p_{3/2}\rightarrow 1d_{5/2}$ single-particle transition, and for the ^{16}O analysis harmonic-oscillator radial wave functions were also used, so we assume a value of $N=1.30$. It should be noted here that in the previous work of Holtkamp *et al.*,[24] an error[34] due to the exclusion of the center-of-mass correction led to values for σ_{DW}^{+} and σ_{DW}^{-} for ^{14}C too small by a factor of 1.25. The corrected value of N appropriate to Ref. 24 then becomes 1.44 ± 0.24, a value consistent with the ^{16}O value of 1.30.

Equations (14) and (20) can now be solved to give Z_0 and Z_1 for the 11.7-MeV state; likewise, Eqs. (14) and (19) give these values for the 17.3-MeV state. The equations are quadratic and give two sets of solutions, but only one set is consistent with the ratio method. The results, shown in Table II, do not include the unknown error on the normalization factor N. For the case of the 17.3-MeV state, the solutions from the ratio method and the cross section method do not quite overlap. This is due to the more accurate treatment of distortion effects and the value of $a=1.93$ (as opposed to $a=2$) used in the cross-section method. Nevertheless, the ratio method clearly singles out the solution with $Z_0<0$.

As already discussed, electron scattering to the 15.2-MeV state is very weak. However, both $(\pi^{+},\pi^{+\prime})$ and $(\pi^{-},\pi^{-\prime})$ cross sections for the excitation of this state have been measured. Thus, Eqs. (19) and (20) can be solved for the two sets of solutions for Z_0 and Z_1 shown in Table II. The first solution set and Eq. (14) give

$$(d\sigma_{\mathrm{peak}}/d\Omega)/(d\sigma_{\mathrm{ESPM}}/d\Omega)=0.022\pm 0.006 ,$$

a value consistent with (e,e') results, while the second set gives an unacceptably large value of

$$(d\sigma_{\mathrm{peak}}/d\Omega)/(d\sigma_{\mathrm{ESPM}}/d\Omega)=0.36\pm 0.03 .$$

In the extreme single-particle model (ESPM), $\Sigma(Z_0^2)_{\mathrm{ESPM}}^{T=1}=1$, and $\Sigma(Z_1^2)_{\mathrm{ESPM}}^{T=1}=\Sigma(Z_1^2)_{\mathrm{ESPM}}^{T=2}=0.5$. As summarized in Table III, the shell-model calculations[1] give $\Sigma(Z_0^2)_{\mathrm{theor}}^{T=1}=0.49$ and $\Sigma(Z_1^2)_{\mathrm{theor}}^{T=1}=0.41$ for the first five predicted $T=1$ states. These five states span the same range in excitation energy as the observed 4^{-} $T=1$ states, and therefore provide a realistic estimate of the expected strength. The remainder of the predicted strength is fragmented among many weak states that fall outside the region studied here. There is just one 4^{-} $T=2$ state predicted within 5-MeV excitation of the observed $T=2$ state, so in this case $\Sigma(Z_1^2)_{\mathrm{theor}}^{T=2}=0.44$. Thus, the measured $T=1$ states exhaust $(41+6)\%$ of the isoscalar strength predicted by the shell model and $(45\pm 2)\%$ of the predicted $T=1$ isovector strength. The $T=2$ state exhausts $(46\pm 4)\%$ of the predicted $T=2$ strength.

F. (p,p') and (p,n) calculations

Now that the Z coefficients have been determined, they can be used to predict the results of other reactions that can be described in terms of the impulse approximation. Before using the Z coefficients to calculate cross sections for charge exchange reactions, we must first multiply them by a ratio of isospin Clebsch-Gordan coefficients [see, for example, Eq. (A21) in Ref. 19]. This ratio is unity for the (p,n) reaction to a $T=1$ state, and $1/\sqrt{3}$ for the (p,n) reaction to a $T=2$ state. As an example, (p,p') and (p,n) cross sections for the 4^{-} states have been calculated, and the results are shown in Fig. 8. These calculations were performed with the nuclear-scattering code DW81 (Ref. 35) using the Love-Franey t-matrix[36] interation and an optical potential[37] based on 200-MeV ^{12}C(p,p) measurements. An incident proton energy of 200 MeV was chosen to correspond to a recent (p,p') experiment.[38]

The (p,p') reaction is sensitive to both the isoscalar and isovector transition amplitudes. In contrast, the (p,n) reaction is purely isovector, and thus the distribution of strengths may be expected to be similar to that seen in the transverse $M4$ electron scattering form factors since they are dominated by the isovector magnetic moments. As can be seen in Fig. 8, all four 4^{-} states, including the 15.2-MeV state, are predicted to be strongly

TABLE III. Experimental and theoretical Z coefficients for the 4^{-} states.

Experimental				Theoretical			
E_x (MeV)	T	Z_0	Z_1	E_x (MeV)	T	Z_0	Z_1
11.7±0.1	1	0.21±0.01	0.32±0.01	12.13	1	0.3667	0.4776
15.2±0.1	1	0.22±0.02	−0.07±0.03	13.50	1	0.3391	0.1717
17.3±0.1	1	−0.32±0.02	0.28±0.01	16.35	1	−0.3279	0.3717
				17.35	1	−0.2143	0.1199
				18.43	1	0.2859	−0.0476
24.4±0.1	2		0.45±0.02	23.92	2		0.6596
				30.51	2		0.0858
				31.97	2		0.1362
				35.00	2		0.0429
				38.00	2		−0.0148

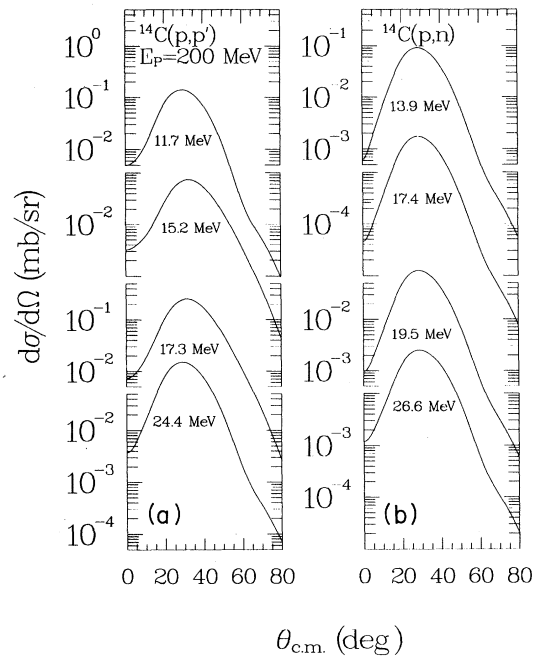

FIG. 8. (a) Calculated (p,p') angular distributions for the 11.7-, 15.2-, 17.3-, and 24.4-MeV 4^- states in ^{14}C. (b) Calculated ^{14}C(p,n) angular distributions to the ^{14}N analogs of the 11.7-, 15.2-, and 17.3-, and 24.4-MeV 4^- states in ^{14}C; the energies in the graph are for the final states in ^{14}N. For both graphs, the incident proton energy is 200 MeV.

excited in (p,p') and the ratios of the calculated cross section maxima, from low to high excitation energies, are 1:0.52:1.8:1.5. As expected, the corresponding ratios for the (p,n) predictions are 1:0.053:0.95:0.76, quite similar to those observed in (e,e').

The forthcoming results from the (p,p') experiment of Ref. 38 should provide a sensitive test of the (p,p') reaction mechanism and of the values of the Z coefficients determined in this paper.

V. OTHER STATES IN ^{14}C

As can be seen in Fig. 3, states at 6.094 ($J^\pi=1^-$), 6.728 (3^-), 7.012 (2^+), and 8.318 (2^+) MeV are strongly excited by 180° (e,e'). Each of these states has been observed in a variety of different experiments, and the excitation energies, spins, and parities are well established. We have also observed strong excitations at 9.84, 10.5, 11.31 and 22.1 MeV. In this section, we present our measured form factors for these levels and briefly compare them with shell-model calculations.

To describe the negative-parity states, we shall adopt the same shell-model calcuations used in the discussion of the 4^- states. For the positive-parity states, calculations were performed in a full $2\hbar\omega$ shell-model space in which the $0s$ core remained inert. The interactions within the p shell, between the p and sd shells, within the sd shell, and between the p and fp shells were the Cohen-Kurath (8–16) 2BME,[39] Millener-Kurath,[1] Kuo-Brown,[40] and Kuo G matrix,[41] respectively. Since the neutrons form a closed core for ^{14}C in a p-shell model, any neutron piece to the excitations discussed here must be attributed to a $2\hbar\omega$ component in the wave function. On the other hand, the protons have a number of configurations available to them within the p shell, and proton excitations need not involve the $2\hbar\omega$ components. Thus, we expect the excitations of the low-lying positive-parity states to be dominantly proton rearrangements within the p shell.

The theoretial predictions are compared to the data by adjusting only the magnitude of the predicted form factor until the best fit is obtained; the normalization factors are collected in Table IV. The harmonic-oscillator parameter has been set to $b=1.60$ fm, roughly midway between the elastic scattering value[42] of 1.71 fm and the $M4$ transition value of 1.52 fm.

A. The 6.094-MeV 1^- state

Data for the excitation of the 6.094-MeV state are shown in Fig. 9 along with the shell-model predictions. In anticipation of a future experiment, we also show the predicted longitudinal form factors, for which no (e,e')

TABLE IV. Normalization factors for theoretical F_T^2. An asterisk indicates an undertermined value.

Observed E_x (MeV)	Predicted E_x (MeV)	$J^\pi T$	Fitted normalization of theoretical F_T^2	Multipolarity of fitted form factor
6.094	6.19	1^-1	0.39±0.05	$E1$
6.728	6.52	3^-1	0.19±0.02	$E3$
7.012	6.84	2^+1	0.75±0.05	$E2$
8.318	7.74	2^+1	1.0±0.07	$E2$
9.84±0.05	10.58,10.36	*	0.2,50	$E1,E3$
10.50±0.05	9.94,13.4	*	0.75,12	$E2,E3$
11.31	9.82	1^+1	0.35±0.02	$M1$
11.7±0.10	12.13	4^-1	0.49±0.03	$M4$
15.2±0.10	13.50	4^-1	<0.64	$M4$
17.3±0.10	16.35	4^-1	0.62±0.04	$M4$
22.1±0.10	22.85	2^-2	0.54±0.06	$M2$
24.4±0.10	23.92	4^-2	0.46±0.04	$M4$

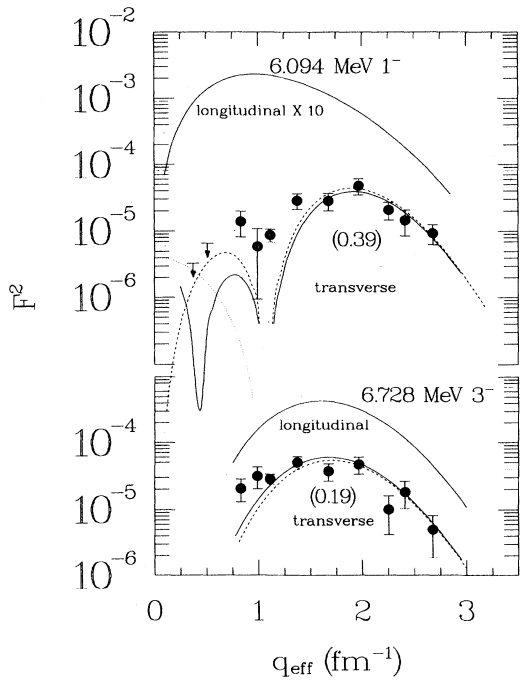

FIG. 9. Top: the 6.094-MeV 1^- inelastic form factor. The upper solid line shows the calculated (Ref. 1) longitudinal form factor and the lower solid line shows the transverse form factor. Dashed and dotted lines show the spin and convection current components of the transverse form factor, respectively. The numbers in parentheses are the normalization factors needed to fit the predicted form factors to the transverse data; no normalization factors have been applied to the calculated longitudinal form factors. Solid circles show present data. Upper limits at $q_{\rm eff}=0.37$ and 0.51 fm^{-1} were estimated from Ref. 43. Bottom: as above, except for excitation of the 6.728-MeV 3^- state.

data are presently available. The magnitude of the predicted transverse form factor has been reduced by a factor of 0.39 to agree with the data. It is evident that its shape is in approximate agreement with the transverse data. This $E1$ form factor is highly model-dependent because of the large number of configurations that can mix to produce vastly different form-factor shapes. Even in the $1\hbar\omega$ space used by Millener and Kurath there are ten possible matrix elements. The five largest predicted[1] matrix element amplitudes are

$$-0.8115(2s_{1/2},p_{1/2})^{\nu}-0.2913(2s_{1/2},p_{3/2})^{\nu}-0.2272(d_{5/2},p_{3/2})^{\nu}-0.1380(d_{3/2},p_{1/2})^{\nu}-0.0936(2s_{1/2},p_{3/2})^{\pi}\ , \quad (21)$$

where ν designates a neutron transition and π designates a proton transition. The first and second matrix elements yield form factors with the same shapes, as do the third and fourth. Mixing among the amplitudes in Eq. (21) can therefore have a large effect on the magnitude of the predicted form factor. This mixing is of course sensitive to the shell-model description of both the ground and excited states, and the work of Huffman *et al.*[44] suggests that the ^{14}C ground state is not adequately described by the standard shell model. Nonetheless, the agreement with the shape of this form factor is encouraging, and the required reduction factor is not inconsistent with those obtained for the 4^- states.

B. The 6.728-MeV 3^- state

Data for the first 3^- state are also shown in Fig. 9. The magnitude of the transverse form factor is again predicted to be too large, this time by about a factor of 5, but again the shape of the predicted form factor is in good agreement with the data. In this case, all of the $E3$ one-body matrix elements which can be obtained in our model space $[(d_{5/2},p_{3/2})_{3^-}$, $(d_{5/2},p_{1/2})_{3^-}$, and $(d_{3/2},p_{3/2})_{3^-}]$ give the same form-factor shape. Interference among these configurations can therefore affect only the magnitude of the form factor. The predicted matrix element amplitudes for this level are

$$0.8622(d_{5/2},p_{1/2})^{\nu}-0.2298(d_{3/2},p_{3/2})^{\nu}+0.1591(d_{5/2},p_{3/2})^{\pi}-0.1328(d_{3/2},p_{3/2})^{\pi}+0.1001(d_{5/2},p_{3/2})^{\nu}+0.0191(d_{5/2},p_{1/2})^{\pi}\ . \quad (22)$$

This state is strongly excited in the ^{13}C(d,p) reactions,[45] giving a spectroscopic factor of 0.65 and supporting the large predicted contribution from the $(d_{5/2},p_{1/2})^{\nu}$ component, consistent with the shell-model predictions. However, it appears from the (e,e') data that there is considerable destructive interference from the other components.

C. The 7.012- and 8.318-MeV 2^+ states

Calculations in a shell-model basis space restricted to the p shell predict[39] just one low-lying 2^+ state at 7.13 MeV, with the second 2^+ state much higher at 15.19 MeV. The structure of the two physical states in ^{14}C at 7.012 and 8.318 MeV is therefore expected to involve components from higher shells, most likely from the *sd* shell. Evidence for *sd*-shell components is found in the results of a ^{12}C$(t,p)^{14}$C experiment,[46] which show that the angular distribution for the ^{14}C ground-state analog in ^{12}C are most accurately reproduced by calculations that include a $(12\pm1)\%$ *sd*-shell admixture in the ^{14}C ground state. Nevertheless, calculations in a $2\hbar\omega$ shell-model space show that the $(p_{1/2},p_{3/2})^{\pi}$ matrix elements still dominate the $E2$ form factors. These form factors therefore test the ability of the calculations to split the p-shell strength between the nominal p-shell state and the $2\hbar\omega$ intruder. The five largest predicted amplitudes for excitation of the 7.012-MeV state are:

$$0.4652(p_{3/2},p_{1/2})^{\pi}-0.0861(p_{3/2},p_{3/2})^{\pi}-0.0478(f_{5/2},p_{1/2})^{\nu}-0.0304(d_{5/2},2s_{1/2})^{\nu}+0.0302(p_{3/2},p_{1/2})^{\nu}\ . \quad (23)$$

and for the 8.318-MeV state, these are

$$-0.2881(p_{3/2},p_{1/2})^{\pi}-0.0723(d_{5/2},2s_{1/2})^{\nu}$$
$$-0.0377(p_{3/2},p_{3/2})^{\pi}+0.0249(p_{3/2},p_{1/2})^{\nu}$$
$$+0.0142(f_{7/2},p_{3/2})^{\pi}\ . \quad (24)$$

The predicted form factors are compared to the experimental data in Fig. 10. Again, the predicted shapes are reasonable as are the overall predicted magnitudes, with only a modest reduction by a factor of 0.75 required for the form factor of the first 2^+ state. No reduction factor is required for the second 2^+ state. There are a few data points at low momentum transfer to define the longitudinal form factors for these 2^+ states, and these data are well described in magnitude by the predicted longitudinal form factors.

Although the transverse (e,e') form factors for these states are almost identical and are well described by the shell-model calculations, evidence from other reactions shows markedly dissimilar structures for these two states. For example, pion-scattering data[23,24] show almost equal $(\pi^+,\pi^{+\prime})$ and $(\pi^-,\pi^{-\prime})$ cross sections for the 7.01-MeV state, yet a $(\pi^+,\pi^{+\prime})/(\pi^-,\pi^{-\prime})$ cross section ratio $R>26$ for the 8.32-MeV state. The $(\pi^+,\pi^{+\prime})$ angular distributions are also markedly different, as are angular distributions from a $^{13}C(d,p)$ experiment.[45] In both the $(\pi^+,\pi^{+\prime})$ and $^{13}C(d,p)$ reactions, the angular distributions were also observed to be significantly different from theoretical predictions. For the case of (π,π'), these results have been interpreted[48] as evidence for strong cancellations between the proton and neutron matrix elements. The $^{13}C(d,p)$ data have been interpreted[45] as evidence for sequential processes through strong stripping to negative-parity states. Clearly, a description of the 7.012- and 8.318-MeV 2^+ states remains an interesting problem in nuclear structure.

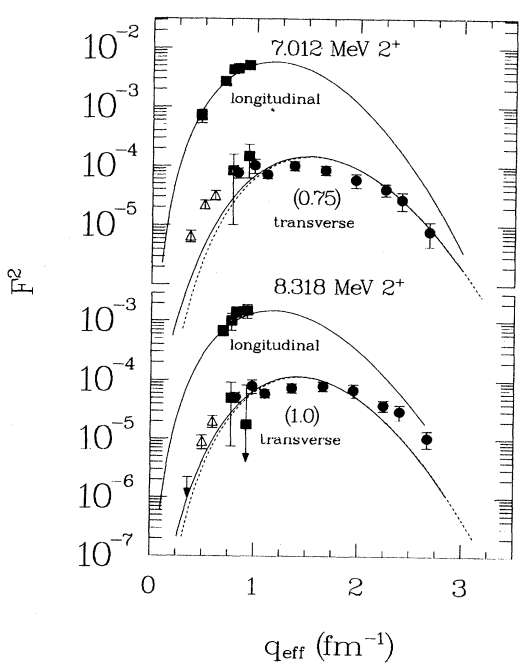

FIG. 10. Form factors for excitation of the 7.012-MeV (top) and 8.318-MeV (bottom) 2^+ states. Labeling is as for Fig. 9, except that solid squares show data from Ref. 47, and open triangles show data from Ref. 43.

D. The 9.84-MeV peak

Based on recent energy-level tabulations,[2,3] the peak observed at 9.83±0.05 MeV consists of unresolved 3^- and 1^- levels at 9.789 and 9.806 MeV, respectively. Results from $^{14}C(\alpha,\alpha')$ and $^{13}C(d,p)$ experiments[45] show no contribution from the 1^- state, and results from a $^{13}C(n,n')$ experiment[3] show the 3^- state to be strongly excited and the 1^- state to be only weakly excited. Fitting the (e,e') form factor with a sum of the second predicted[1] $E1$ ($E_x=10.58$ MeV) and $E3$ ($E_x=10.36$ MeV) form factors yields the curves shown in Fig. 11. The fitted normalization factors for the $E1$ and $E3$ form fac-

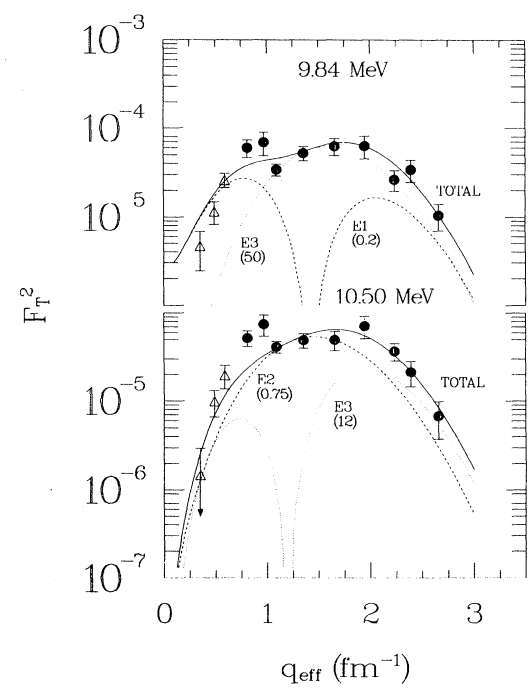

FIG. 11. Form factors for the 9.84-MeV peak (top) and the 10.50-MeV peak (bottom). Solid circles represent the present data and the open triangles represent the data from Ref. 43. For the 9.84-MeV peak, the dashed line shows the second predicted (Ref. 1) $E1$ form factor while the dotted line shows second predicted (Ref. 1) $E3$ form factor. The solid line shows the sum of these two form factors (including the normalization factors shown). For the 10.50-MeV peak, the dashed line shows the third predicted $E2$ form factor while the dotted line shows the third predicted (Ref. 1) $E3$ form factor. The solid line shows the sum of these two form factors (again including the normalization factors shown).

tors are 0.2 and 50, respectively. For the $E1$ transition, the five largest predicted[1] amplitudes are

$$0.5329(2s_{1/2},p_{3/2})^{\nu}-0.3723(2s_{1/2},p_{1/2})^{\nu} -0.1400(2s_{1/2},p_{3/2})^{\pi}-0.1070(p_{1/2},s_{1/2})^{\pi} -0.0795(d_{3/2},p_{3/2})^{\nu}\ , \quad (25)$$

and for the $E3$ transition, the five largest predicted amplitudes are

$$-0.6939(d_{5/2},p_{3/2})^{\nu}+0.1014(d_{3/2},p_{3/2})^{\nu} +0.0909(d_{5/2},p_{1/2})^{\nu}+0.0552(d_{3/2},p_{3/2})^{\pi} -0.0171(d_{5/2},p_{3/2})^{\pi}\ . \quad (26)$$

It is unlikely that the 1^- state will be weakly excited by the (n,n'), (α,α'), and (d,p) reactions and strongly excited by the (e,e') reaction. The $E3$ normalization factor is also unreasonably large, due to a strong suppression of the calculated form factor arising from a delicate cancellation between the various terms of Eq. (26). Thus it appears that these two states, which are expected to make up this peak, are simply poorly described by the present shell-model calculations. In fact, angular distributions predicted for the (d,p) and (α,α') reactions deviate from the observed cross sections for angles greater than about the half-maximum of the first peak in the angular distribution,[45] also suggesting a structure in disagreement with that predicted by the shell model.[1]

E. The 10.5-MeV peak

Three separate staes have been identified in the vicinity of the peak observed at 10.5±0.1 MeV. The recent compilation by Ajzenberg-Selove[2] concludes there are $J^{\pi}=2^+$, $\geq 1^{\pm}$, and (3^-) levels at $E_x=10.425$-, 10.449-, and 10.498-MeV excitation, respectively. The angular distribution for a peak observed at 10.50-MeV excitation in ^{14}C(π,π') (Refs. 23 and 49) is well described as an $E2$ transition. However, the (e,e') form factor at low q is not well described by the predicted $E2$ form factor, as shown in Fig. 11. To address the possibility that the observed form factor is actually comprised of a sum of $E2$ and $E3$ form factors, the magnitudes of the predicted[1] $E2$ ($E_x=9.94$ MeV) and $E3$ ($E_x=13.11$ MeV) form factors have been adjusted to fit the data, as shown in Fig. 11. For the $E2$ transition, the five strongest predicted matrix elements are

$$0.1999(p_{3/2},p_{1/2})^{\pi}+0.1576(d_{5/2},d_{5/2})^{\nu} -0.0672(p_{3/2},p_{1/2})^{\nu}-0.0373(d_{5/2},2s_{1/2})^{\nu} +0.0200(p_{3/2},p_{3/2})^{\nu}\ , \quad (27)$$

and for the $E3$ transition, the five strongest predicted[1] matrix elements are

$$0.2179(d_{5/2},p_{3/2})^{\pi}+0.1360(d_{5/2},p_{3/2})^{\nu} -0.1163(d_{3/2},p_{3/2})^{\pi}-0.0904(d_{5/2},p_{1/2})^{\nu} -0.0725(d_{3/2},p_{3/2})^{\nu}\ . \quad (28)$$

The $E2$ normalization factor of 0.75 is reasonable, but the $E3$ normalization factor of 12 is unrealistic. However, we note that the normalization factor is poorly determined by the data, leading to a large uncertainty in the $E3$ normalization factor. The $E3$ form factor also has the wrong shape to explain a low-q enhancement. We conclude that the peak observed in this work is most likely dominated by a $J^{\pi}=2^+$ state, but may still have contributions from other states of unknown multipolarity.

F. The 11.31 MeV 1^+ state

The quenching of observed $M1$ strength throughout the periodic table has been of interest for some time.[50,51] Delta-hole admixtures, multi-$\hbar\omega$ excitations, and other exotic effects have been proposed as mechanisms to explain this effect. Sometimes the strength is fragmented into many states,[52] while at other times the strength is concentrated into a single state, as happens for the 1^+ states in ^{12}C and ^{14}C. In the extreme single-particle shell-model description of ^{12}C and ^{14}C, the 1^+ states are described by pure isovector and pure proton $(p_{1/2},p_{3/2}^{-1})$ transitions, respectively. However, form factors generated from each of these pure transitions fail to describe the shape of the observed form factors. Shell-model calculations in a $2\hbar\omega$ space also predict a predominantly $p_{3/2}\rightarrow p_{1/2}$ proton transition in ^{14}C, and once again these calculations fail to describe the measured form factor, as shown in Fig. 12. For this $M1$ transition, the five strong-

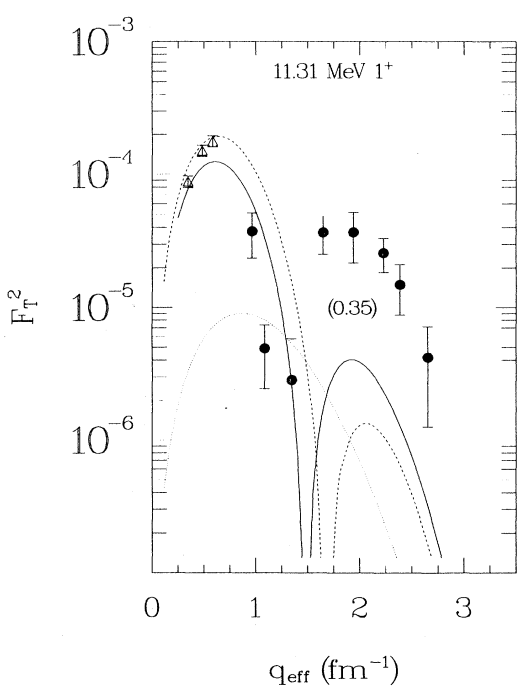

FIG. 12. Form factor for excitation of the ^{14}C 11.31-MeV 1^+ state. Solid circles represent the present data and open triangles show data from Ref. 43. The solid line is the fit of the predicted form factor to data. The dashed and dotted lines show the spin and convection current components of the transverse form factor, respectively. The overall normalization factor applied to the predicted form factor is shown in parentheses.

est predicted transition amplitudes are

$$-0.6006(p_{3/2},p_{1/2})^{\pi}+0.0352(f_{5/2},p_{3/2})^{\nu} -0.0228(2p_{3/2},p_{3/2})^{\pi}-0.0218(d_{5/2},d_{3/2})^{\pi} -0.0109(d_{5/2},d_{3/2})^{\nu} . \quad (29)$$

Significant mixing between the neutron and proton matrix elements, i.e., more strength outside the p shell, is probably needed to describe the observed form factors.

G. The (12–17)-MeV region of excitation

Seven weakly excited peaks at 12.20, 12.86, 13.62, 14.03, 14.92, 15.96, and 16.53 MeV consistently appear in the (e,e') spectra, but have cross sections at the limits of the sensitivity of this experiment. Except for the 12.86- and 15.96-MeV peaks, the observed form factors do not have well-defined shapes, as shown in Fig. 13. The (12.86±0.10)-MeV peak may be identified with a previously observed[3] level at 12.87 MeV with possible $J^{\pi}=2^{+}$, 3^{-}, $4^{\pm}$, or $5^{\pm}$. The peak at 15.96 MeV has not been observed in previous work.[2,3,45] Peaks at 12.20±0.10, 13.62±0.10, and 14.92±0.10 MeV may be identified with levels observed at 12.22 ($J^{\pi}=1^{-}$),[3] 13.58 (1^{-}),[2] and 14.82 (3^{-}) MeV, respectively.[45] Peaks at 14.03±0.10 and 16.53±0.10 MeV cannot be readily identified with any previously observed levels.

H. The 22.1-MeV 2^{-} state

This state is a strong candidate for the isobaric analog to the 2^{-}, $T=2$ ground state of ^{14}B. As shown in Fig. 14, the shape of the form factor is well described by shell-model calculations,[1] although the predicted magnitude is almost a factor of 2 too high. Interference between the $(2s_{1/2},p_{3/2})_{M2}$ and $(d_{5/2},p_{3/2})_{M2}$ matrix elements produces a form factor that is peaked at high momentum transfer explaining why earlier searches at low q for this state were unsuccessful.[53] Although the shape of this $M2$ form factor is similar to that for an $M3$ or $M4$ transition, no 3^{+} or 4^{-} states are predicted to lie near this excitation energy, thus permitting a degree of confidence in this identification.

From the excitation energy of this state, the ^{14}B mass excess,[25] the ^{14}C mass excess,[54] and he neutron-proton mass difference Δ_{np}, the ^{14}B-^{14}C Coulomb energy difference is calculated to be

$$\begin{aligned}\Delta E_c &= M_{Z>}-M_{Z<}+\Delta_{np}\\ &=[3.020+(22.1\pm0.10)]\\ &\quad-(23.657\pm0.030)+(0.782)\\ &=2.25\pm0.10\ \text{MeV}\ ,\end{aligned} \quad (30)$$

a value close to the 2.47 MeV given by the semiemprical mass formula.[55]

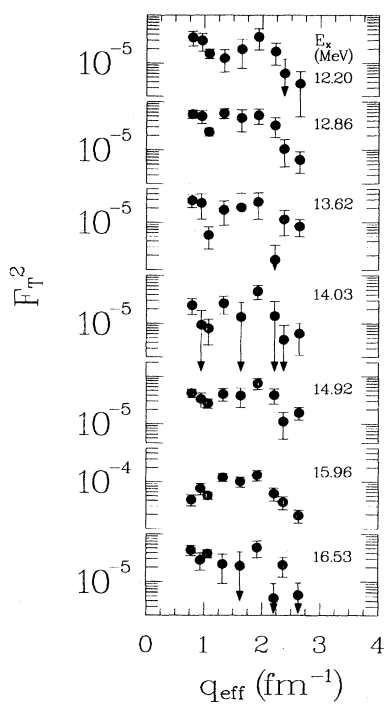

FIG. 13. Form factors extracted for the 12.20-, 12.86-, 13.62-, 14.03-, 14.92-, 15.96-, and 16.53-MeV peaks.

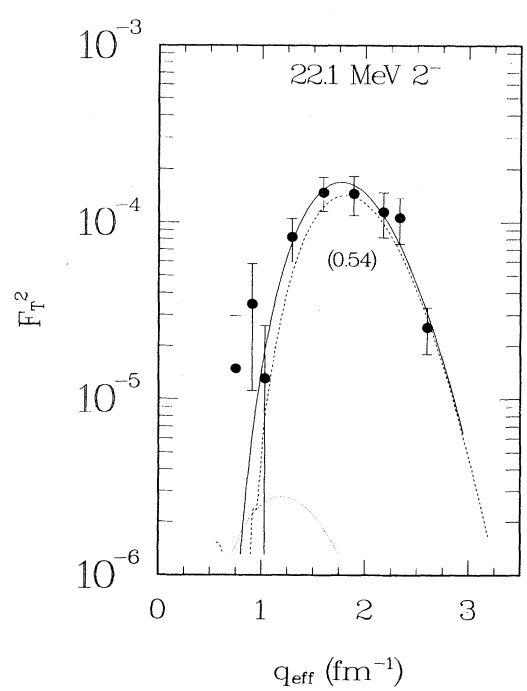

FIG. 14. Form factor for excitation of the 22.1-MeV 2^{-} state, a candidate for the analog to the ^{14}B ground state. Labeling of the curves is as in Fig. 12.

VI. CONCLUSIONS

Because the stretched $(d_{5/2},p_{3/2})$ spin matrix element is expected to be the only important contribution to $M4$ excitations in p-shell nuclei, a rather definitive test of shell-model predictions is possible for the 4^- states in ^{14}C. The analysis of our data shows that only roughly one-half of the $M4$ strength expected from these calculations is observed in each state. Furthermore, a combined analysis of (e,e') and (π,π') data, which allowed us to separate the isoscalar and isovector contributions to the excitation of the 4^- $T=1$ states, shows that the observed isoscalar strength is about the same as the observed isovector strength and that the shell model overpredicts both.

This missing strength may be partly understood in terms of sd-shell components in the ^{14}C ground state. In the $M4$ calculations,[1] the ^{14}C ground state was assumed to be well described within the p shell. However, results from a ^{12}C(t,p) experiment[46] show that $(12\pm1)\%$ of the ^{14}C ground state involves sd shell components. Furthermore, a recent analysis[44] of electron scattering to the analog of the ^{14}C ground state in ^{14}N (at 2.31 MeV) required a nontraditional p-shell description for this state. Including such ingredients would tend to reduce and fragment the predicted $(d_{5/2},p_{3/2})_{M4}$ strength, and would result in peaks that would be too weak to be observed.

The transverse form factors for other unnatural-parity states are more complex because of contributions from both spin and orbital transition densities and from competing shell-model configurations, but again we found that the shell model consistently overpredicted the strength of the form factors. For example, a large quenching factor of 0.35 was required in order to fit the first maximum of the $M1$ form factor, while the form factor in the region of the second maximum was too weak by a factor of 10. Although the shape of the $M2$ transverse form factor for the 22.1-MeV state, which is the previously sought after analog to the 2^- ^{14}B ground state, is well described by the calculations, a reduction factor of 0.54 is required in order to fit the magnitude of the form factor.

The transverse form factors for the low-lying natural-parity states such as the 6.094 (1^-), 6.728 (3^-), 7.012(2^+), and 8.318 (2^+) states are also expected to be complicated. Although the shapes of these form factors were generally well described by the shell-model calculations, the model predicted too much strength for the three lowest excited states. The calculations did reproduce the strength for the 8.318-MeV state fairly well even though this state is thought to be a mixture between a p-shell state and an $(sd)^2$ "intruder." In order to further test the shell-model wave functions for these natural-parity states, measurements of the Coulomb form factors would be very valuable in discerning the proton contributions which are expected to be weak in the 6.094- and 6.718-MeV excitations, but strong in the 7.012- and 8.318-MeV excitations. It would be interesting to see how the systematics of a comparison of measured Coulomb form factors with those predicted by the shell-model calculations are similar to those we have seen here for the transverse form factors.

ACKNOWLEDGMENTS

M.A.P., R.A.L., J.D., R.S.H., R.L.H., B.P., and G.A.P. acknowledge support from the U.S. Department of Energy. J.A., J.L., and M.A.M. acknowledge support from the U.S.-Israel Binational Science Foundation (BSF-Jerusalem).

---

*Present address: MP5, MS H838, Los Alamos National Laboratory, Los Alamos, NM 87545.

†Present address: Department of Physics, University of Virginia, Charlottesville, VA 22901.

‡Present address: Department of Physics, Wittenberg University, Springfield, OH 45501.

§Present address: Department of Physics, Northwestern University, Evanston, IL 60201.

[1]D. J. Millener and D. Kurath, Nucl. Phys. **A255**, 315 (1975); D. J. Millener, private communication.

[2]F. Ajzenberg-Selove, Nucl. Phys. **A449**, 1 (1986).

[3]R. O. Lane, H. D. Knox, and P. Hoffmann-Pinter, Phys. Rev. C **23**, 1883 (1981).

[4]M. A. Plum, R. A. Lindgrem, J. Dubach, R. S. Hicks, R. L. Huffman, J. Alster, J. Lichtenstadt, M. A. Moinester, and H. Baer, Phys. Lett. **137B**, 15 (1984).

[5]R. S. Hicks, R. A. Lindgren, M. A. Plum, G. A. Peterson, H. Crannell, D. I. Sober, H. A. Thiessen, and D. J. Millener, Phys. Rev. C **34**, 1161 (1986).

[6]See AIP document No. PAPS PRVCA 40-1861-15 for 15 pages of tabulated cross-section measurements. Order by PAPS number and journal reference from American Institute of Physics, Physics Auxiliary Publication Service, 335 East 45th Street, New York, NY 10017. The price is $1.50 for microfiche (98 pages) or $5.00 for photocopies of up to 30 pages, and $0.15 for each additional page over 30 pages. Airmail additional. Make checks payable to American Institute of Physics.

[7]G. A. Peterson, J. B. Flanz, D. V. Webb, H. DeVries, and C. F. Williamson, Nucl. Instrum. Methods **160**, 375 (1979).

[8]W. Bertozzi, M. V. Hynes, C. P. Sargent, W. Turchinetz, and C. Williamson, Nucl. Instrum. Methods **162**, 211 (1979).

[9]W. Bertozzi, M. V. Hynes, C. P. Sargent, C. Creswell, P. C. Dunn, A. Hirsch, M. Leitch, B. Norum, F. N. Rad, and T. Sasanuma, Nucl. Instrum. Methods **141**, 457 (1977).

[10]C. J. Harvey, H. W. Baer, J. A. Johnstone, C. L. Morris, S. J. Seestrom-Morris, D. Dehnhard, D. B. Holtkamp, and S. J. Greene, Phys. Rev. C **33**, 1454 (1986).

[11]An alloy of nickel, steel, and cobalt produced by Hamilton Precision Metals, Lancaster, PA 17604.

[12]Computer code ESFIT, written by R. S. Hicks from formalism developed by P. Auer and J. Bergstrom [I. P. Auer and J. C.

Bergstrom, University of Saskatchewan, FORTRAN program IPA, unpublished notes (1975)]. See also R. S. Hicks, A. Hotta, J. B. Flanz, and H. deVries, Phys. Rev. C **21**, 2177 (1980).

[13]P. R. Bevington, *Data Reduction and Error Analysis for the Physical Sciences* (McGraw-Hill, New York, 1969).

[14]G. W. Phillips, Nucl. Instrum. Methods **153**, 449 (1978).

[15]D. G. Ravenhall and D. R. Yennie, Proc. Phys. Soc. London A **70**, 857 (1957).

[16]L. A. Schaler, L. Schellenberg, T. Q. Phan, G. Piller, A. Ruetschi, and H. Schneuwly, Nucl. Phys. **A379**, 523 (1982).

[17]F. Petrovich, R. J. Philpott, J. W. Carr, and A. W. Carpenter, Nucl. Phys. **A425**, 609 (1984).

[18]R. A. Lindgren and F. Petrovich, *Spin Excitations in Nuclei,* edited by F. Petrovich (Plenum, New York, 1984), p. 323.

[19]F. Petrovich, R. H. Howell, C. H. Poppe, S. M. Austin, and G. M. Crawley, Nucl. Phys. **A383**, 355 (1982).

[20]G. G. Simon, Ph.D. thesis, University of Mainz, West Germany, 1978, p. 67, fit $F1$.

[21]T. deForest and J. D. Walecka, Adv. Phys. **15**, 1 (1966).

[22]R. S. Hicks, J. B. Flanz, R. A. Lindgren, G. A. Peterson, L. W. Fagg, and D. J. Millener, Phys. Rev. C **30**, 1 (1984).

[23]D. B. Holtkamp, S. J. Seestrom-Morris, S. Chakravarti, D. Dehnhard, H. W. Baer, C. L. Morris, S. J. Greene, and C. J. Harvey, Phys. Rev. Lett. **47**, 216 (1981).

[24]D. B. Holtkamp, S. J. Seestrom-Morris, D. Dehnhard, H. W. Baer, C. L. Morris, S. J. Greene, C. J. harvey, D. Kurath, and J. A. Carr, Phys. Rev. C **31**, 957 (1985).

[25]G. C. Ball, C. J. Costa, W. G. Davies, J. S. Foster, J. C. Hardy, and A. B. McDonald, Phys. Rev. Lett. **31**, 395 (1973).

[26]H. W. Baer, J. A. Bistirlich, K. M. Crowe, W. Dahme, C. Joseph, J. P. Perroud, M. Lebrun, C. J. Martoff, U. Straumann, and P. Truöl, Phys. Rev. C **28**, 761 (1983).

[27]C. E. Hyde-Wright, Ph.D. thesis, Massachusetts Institute of Technology, 1984.

[28]H. Zarek, S. Yen, B. O. Pich, T. E. Drake, C. F. Williamson, S. Kowalski, and C. P. Sargent, Phys. Rev. C **29**, 1664 (1984).

[29]B. L. Clausen, R. J. Peterson, and R. A. Lindgren, Phys. Rev. C **38**, 589 (1988).

[30]J. A. Carr, F. Petrovich, D. Halderson, and J. J. Kelly, code ALLWRLD (unpublished).

[31]J. A. Carr, code MSUDWPI (unpublished), adapted from the code DWPI, R. A. Eisenstein and G. A. Miller, Comput. Phys. Commun. **11**, 95 (1976).

[32]J. A. Carr, F. Petrovich, D. Halderson, D. B. Holtkamp, and W. B. Cottingame, Phys. Rev. C **27**, 1636 (1983).

[33]G. Rowe, M. Salomon, and R. H. Landau, Phys. Rev. C **18**, 584 (1978).

[34]J. A. Carr, private communication.

[35]Program DWBA70, R. Shafer and J. Raynal (unpublished); extended version DW81 by J. R. Comfort (unpublished).

[36]M. Franey and G. Love, Phys. Rev. C **31**, 488 (1985).

[37]H. Meyer, P. Schwandt, G. L. Moake, and P. P. Singh, Phys. Rev. C **23**, 616 (1981).

[38]A. D. Bacher, G. T. Emery, C. Olmer, W. Jones, D. W. Miller, H. Nann, E. J. Stephenson, R. A. Lindgren, and M. A. Plum, Indiana University Cyclotron Facility Research Proposal 82-23, 1982.

[39]S. Cohen and D. Kurath, Nucl. Phys. **A73**, 1 (1965).

[40]T. T. S. Kuo and G. E. Brown, Nucl. Phys. **A85**, 40 (1966).

[41]T. T. S. Kuo, private communication.

[42]F. J. Kline, H. Crannell, J. T. O'Brien, J. McCarthy, and R. R. Whitney, Nucl. Phys. **A209**, 381 (1973).

[43]H. Crannell, J. M. Finn, P. Hallowell, J. T. O'Brien, N. Ensslin, L. W. Fagg, E. C. Jones, Jr., and W. L. Bendell, Nucl. Phys. **A278**, 253 (1977).

[44]R. L. Huffman, J. Dubach, R. S. Hicks, and M. A. Plum, Phys. Rev. C **35**, 1 (1987).

[45]R. J. Peterson, H. C. Bhang, J. J. Hamill, and T. G. Masterson, Nucl. Phys. **A425**, 469 (1984).

[46]H. T. Fortune and G. S. Stephans, Phys. Rev. C **25**, 1 (1982).

[47]H. Crannell, P. L. Hallowell, J. T. O'Brien, J. M. Finn, F. J. Kline, S. Penner, J. W. Lightbody, Jr., and S. P. Fivozinsky, Supplement of Research Report of Laboratory of Nuclear Science, Vol. 5, Tohoku University, Sendai, Japan, 1972.

[48]D. Dehnhard, Nucl. Phys. **A374**, 377 (1982).

[49]M. K. Garakani, Master's thesis, University of Minnesota, 1984.

[50]L. W. Fagg, Rev. Mod. Phys. **47**, 683 (1975).

[51]W. Knupfer, M. Dillig, and A. Richter, Phys. Lett. **95B**, 349 (1980).

[52]R. S. Hicks and G. A. Peterson, in *Spin Excitations in Nuclei,* edited by F. Petrovich *et al.* (Plenum, New York, 1984), p. 47.

[53]F. J. Kline, H. Crannell, J. M. Finn, P. L. Hallowell, J. T. O'Brien, C. W. Werntz, S. P. Fivozinsky, J. W. Lightbody, Jr., and S. Penner, Nuovo Cimento **23A**, 137 (1974).

[54]A. H. Wapstra and N. B. Gove, Nucl. Data, Sect. A **9**, 265 (1971).

[55]P. Marmier and E. Sheldon, in *Physics of Nuclei and Particles* (Academic, New York, 1969), p. 880.